Computers and Chemical Engineering 61 (2014) 20–29

Contents lists available at ScienceDirect

Computers and Chemical Engineering

journal homepage: www.elsevier.com/locate/compchemeng

An effective procedure for sensor variable selection and utilization in plasma etching for semiconductor manufacturing

Kye Hyun Baek[a,b], Thomas F. Edgar[c], Kiwook Song[b], Gilheyun Choi[a], Han Ku Cho[a], Chonghun Han[b,d,e,*]

[a] Semiconductor R&D Center, Samsung Electronics Co., Ltd, San #16 Banwol-Dong, Hwasung-City, Gyeonggi-do 445-701, Republic of Korea
[b] School of Chemical and Biological Engineering, Seoul National University, San 56-1, Shillim-dong, Kwanak-gu, Seoul 151-742, Republic of Korea
[c] Department of Chemical Engineering, University of Texas at Austin, 1 University Station C0400, Austin, TX 78712, USA
[d] Institute of Chemical Processes, Seoul National University, San 56-1, Shillim-dong, Kwanak-gu, Seoul 151-742, Republic of Korea
[e] Engineering Research Institute, Seoul National University, San 56-1, Shillim-dong, Kwanak-gu, Seoul 151-742, Republic of Korea

ARTICLE INFO

Article history:
Received 26 November 2012
Received in revised form
11 September 2013
Accepted 20 September 2013
Available online 24 October 2013

Keywords:
Variable selection
Integrated squared response
Plasma etching
Multivariable control
Virtual metrology
Relative gain array

ABSTRACT

Plasma etching processes have a potentially large number of sensor variables to be utilized, and the number of the sensor variables is growing due to advances in real-time sensors. In addition, the sensor variables from plasma sensors require additional knowledge about plasmas, which becomes a big burden for engineers to utilize them in this filed. Thus an effective procedure for sensor variable selection with minimum plasma knowledge is needed to develop in plasma etching. The integrated squared response (ISR) based sensor variable selection method which facilitates collecting and analyzing sensor data at one time with regard to manipulated variables (MVs) is suggested in this paper. The reference sensor library as well as sensor ranking tables constructed on the basis of ISR can give insight into plasma sensors. The ISR based sensor variable selection method is incorporated with relative gain array (RGA) or non-square relative gain array (NRGA) for effective variable selection in building a virtual metrology (VM) system to predict critical dimension (CD) in plasma etching. The application of the technique introduced in this paper is shown to be effective in the CD prediction in plasma etching for a dynamic random access memory (DRAM) manufacturing. The procedure for sensor variable selection introduced in this paper can be a starting point for various sensor-related applications in semiconductor manufacturing.

1. Introduction

In today's semiconductor manufacturing environment, many in situ sensors are employed for monitoring plasma etch equipment operation and process results due to the inherent complexity of plasmas (Baek et al., 2005; Chen, Huang, Spanos, & Gatto, 1996; Klick, Rehak, & Kammeyer, 1997; Park, Grimard, & Grizzle, 2003; Sobolewski, 2006; Yue, Qin, Markle, Nauert, & Gatto, 2000). The potential number of measurements in plasma etching is greater than several hundred. Despite the large number of existing sensors, process and equipment engineers in plasma processing continue to evaluate newly developed state-of-the-art sensors because they believe that current sensors do not provide enough information about plasma states. Therefore, the number of in situ sensors in plasma processes is expected to increase, which provides an incentive to develop an effective procedure for sensor variable selection and utilization.

Because plasma etch processes are complex multivariable processes, manipulated variables (MVs) can be adjusted considering state variables (SVs) and performance variables (PVs). Since SVs measure hardware and plasma states through various in situ sensors, their proper utilization is invaluable for process set-up, process and equipment control, and fault detection. However, utilization of SVs in practice is limited because interpretation of them regarding MVs and PVs requires additional knowledge. Therefore, a general and efficient approach to selecting proper SVs and their utilization needs to be developed.

This paper discusses an effective procedure for sensor variable selection and utilization in plasma etching. Firstly, several issues in sensor variable selection for plasma etching will be addressed in terms of complexities of plasma etch processes, variety of in situ sensors and scaling issues. Then, in Section 3, brief theory overview which is suggested in this paper will be made. In Section 4, the results applied in a critical dimension (CD) virtual metrology (VM) for manufacturing a dynamic random access memory will be shown, which proves the effectiveness of our methodology. The proposed sensor variable selection technique can be utilized as a starting point in building a reference sensor library for fault

* Corresponding author. Tel.: +82 2 880 1887; fax: +82 2 873 2767.
E-mail address: chhan@snu.ac.kr (C. Han).

0098-1354/$ – see front matter © 2013 Elsevier Ltd. All rights reserved.
http://dx.doi.org/10.1016/j.compchemeng.2013.09.016

detection and classification, evaluating sensor performance, and selecting MVs–PVs for equipment control. Hopefully, the results in this paper will encourage development of general, user-friendly sensor variable selection techniques for process and equipment engineers.

2. Issues in sensor variable selection for plasma etching processes

2.1. Complex multivariate plasma etch process

Plasma etching is a key process together with photolithography for patterning in semiconductor manufacturing (Lieberman & Lichtenberg, 2005). This process uses a plasma to generate highly reactive ionized species from relatively inert molecular gases to remove material from surfaces. The ionized species are accelerated in a perpendicular direction to wafer by the sheath potential of the plasma, which enables performing anisotropic etching processes. However, the plasma etch processes are complicated due to the inherent complexity of plasmas. That is, in addition to the physical and chemical reactions in plasma etching, the electrical interaction between charged particles and the electromagnetic fields within the plasma, which can be reflected to plasma state variables from plasma sensors, are not simple to interpret. Therefore, plasma etch processes must consider plasma state variables together with input and output variables to better understand their processes.

Fig. 1 illustrates the three groups of variables in a plasma etch process, where the plasma is a medium connecting MVs and PVs with several hundred SVs. Until recent years, a group of equipment state variables from built-in hardware gauges have been mainly utilized for equipment monitoring and process readiness check. However, with the narrower process window due to the semiconductor device shrinkage, the detection capability of those SVs is now insufficient to measure process performance. As a result, plasma state variables from plasma sensors, which are more representative of process results, are emerging as alternatives. Utilization of plasma state variables, however, is limited because it requires additional knowledge to interpret in terms of their relationships to MVs and PVs. In addition, the limited number of plasma sensors currently available in an industrial environment makes this situation worse because of the lack of information on the plasma. Therefore, the number of new plasma sensors will continue to increase and with the increased number, an efficient and affordable sensor variable selection and utilization technique needs to be developed in plasma etch processes.

2.2. Various sensor variables in plasma etching equipment

The schematic of the plasma etching equipment and additional in situ sensors employed in this paper is shown in Fig. 2. The etching equipment is an inductively coupled plasma reactor from Applied Materials, Inc., which uses the rf power of 13.56 MHz to generate plasma through inductive coupling and has optical emission spectroscopy (OES) and VI-probe built in the equipment. The OES sensor measures emission spectra ranging from 200 nm to 800 nm, which reflects chemical properties in plasma (Coburn & Chen, 1980). The VI-probe sensor measures the voltage, current and phase of the rf power of 13.56 MHz and its harmonics, with which the sheath potential of plasma can be estimated (Semmler, Awakowicz, & Keudell, 2007). The self-excited electron resonance spectroscopy (SEERS) from Plasmetrex GmbH is an additionally installed sensor, which measures electrical and chemical properties of the plasmas such as electron density, and electron collision rate, and so on (Baek et al., 2005; Klick, 1996; Klick et al., 1997). The other sensors that monitor equipment states like pressure and temperature are not shown in Fig. 2, but they are also evaluated together in this paper.

Table 1 lists sensor variable categories employed in this paper, which shows the total number of sensor variables is 1308 and each sensor variable has the different physical properties. As discussed in Section 2.1, the total number of sensor variables in plasma etching has been continually growing, so their proper utilization will be difficult if effective variable selection techniques do not exist.

2.3. Variable selection through principal component analysis

Principle component analysis (PCA) is a mathematical procedure that uses orthogonal transformation. It convert a set of observations of possible correlated variables into a set of values of linearly uncorrelated variables called principal components (Jolliffe, 2002; Wold, Esbensen, & Geladi, 1987). This transformation is defined in such a way that the first principle component accounts for as much of the variability in the data as possible and each subsequent component in turn has the highest variance possible under the constraint that it should be orthogonal to the preceding components. Often, its operation can be thought of as revealing the internal structure of the data in a way that best explains the variance in the data. Thus the loading of the first PC can be analyzed in terms of importance of sensor variables which accounts for the variability of the data set.

PCA is sensitive to the scaling of the variables. This might lead to arbitrary decision of sensor selection in plasma etching where more than hundreds sensor variables with different physical properties exist like that shown in Table 1. Fig. 3 illustrates how the weightings of each sensor variables in the loading vector of the first PC are changing according to scaling methods of the data set in plasma etching. For example, the negatively or positively highest weighting sensor variable is changed from sensor variable number 250 in the no-scale case to sensor variable number 122 in the mean centered case, or to sensor variable number 100 in the mean centered and unit variance case. Therefore, unless any additional techniques about scaling is built in PCA to handle the scaling issue, the statistic based PCA cannot be applied to sensor variable selection in plasma etching. In addition, relaying on the statistics without considering physical properties of sensor variables may lead to a wrong decision in plasma etching where nonlinear behavior of plasma governs reaction of process. Thus an affordable sensor variable selection technique which can reflect physical properties of sensor variables and analyze the interaction between variables within a plasma needs to be develop in plasma etching processes.

3. Brief theory overview

3.1. Integrated squared response (ISR) based sensor variable selection method

Under the consideration of the circumstances in sensor variable selection described in Section 2, several factors should be taken into account in plasma etching. The first factor is the heterogeneity of SVs. This comes from various sensors to measure plasma characteristics and equipment states as well and might cause scaling issues of variables due to the different unit and sensitivity of each sensor variable. The second factor is the redundancy in the data. This might cause the collinearity issues which lead to numerical instabilities in calculation and poor prediction performance in regression modeling. The third factor is the presence of interactions and non-linearities among SVs due to the inherent complexity of the plasmas. Therefore, a new variable selection method should be developed for plasma etching processes in such a way to minimize the bad effects from the factors above.

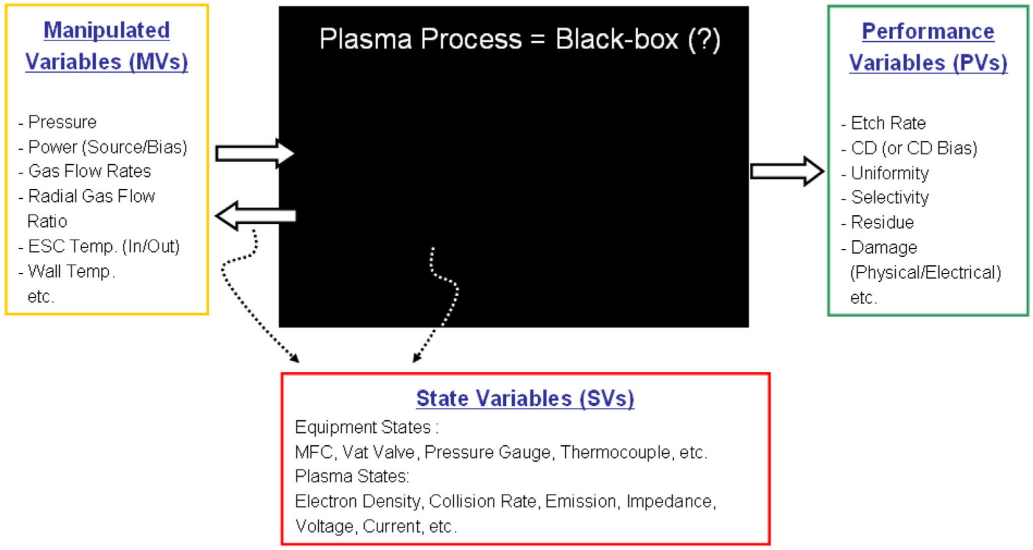

Fig. 1. Overview of complex multivariable plasma etch processes whose variables are classified into manipulated variables, state variables, and performance variables.

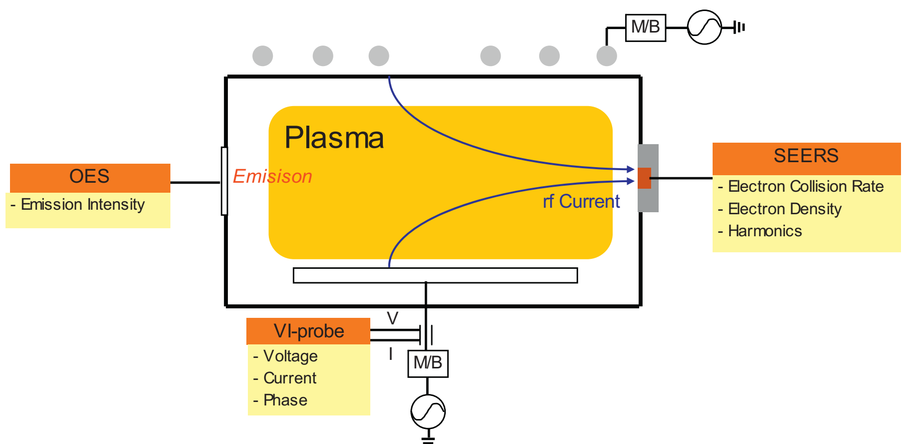

Fig. 2. Schematic of the plasma etching system and additional in situ sensors employed in this paper.

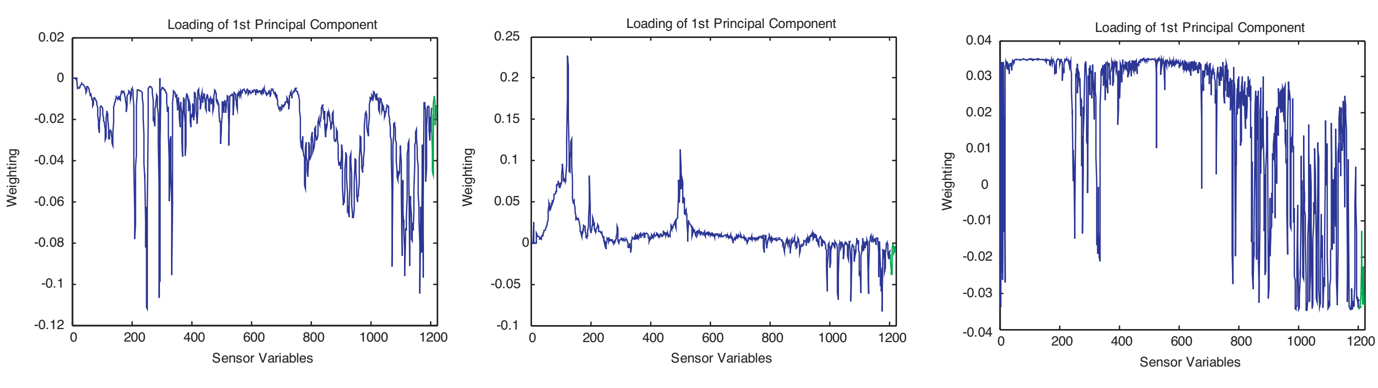

Fig. 3. Loadings of the first PC according to scaling methods: (a) no scaling, (b) mean centered, and (c) mean centered and unit variance.

A sensor variable ranking table, which sorts all sensor variables in a descending order in terms of each MV, would be useful as a starting point in variable selection. This is because the process results in plasma etching are closely related to SVs and SVs are manipulated by MVs. The sensor variable ranking table should be obtained after the entire sensor responses to each MV are analyzed, which takes large amount of time and knowledge. Given this situation, a systematic procedure to collect and analyze the entire sensor responses would be desirable.

As a systematic procedure for sensor data collection and analysis, a time-integrated variance calculation method with a step change test is suggested in this paper. By running the one recipe like that summarized in Table 2, the entire sensor response data for each MV can be collected at one time. To make sure that each

Table 1
List of sensor variables employed in this paper.

Hardware gauges		SEERS		VI-probe		OES	
Variables	Description	Variables	Description	Variables	Description	Variables	Description
Throttle current_pct_open	Throttle valve open level	Collision rate	Electron collision rate	f0V	Fundamental voltage	200.0 nm	Emission intensity
Source forward_reading	Forward power reading	Electron density	Electron density	f0I	Fundamental current	200.5 nm	Emission intensity
Source reflected_reading	Reflected power reading	1st Harmonics	1st harmoncs current	f0Phase	Fundamental phase	201.0 nm	Emission intensity
Source series_reading	Matchbox reading (Series Cap.)	2nd Harmonics	2nd harmonics current	f1V	1st harmonics voltage	201.5 nm	Emission intensity
Source shunt_reading	Matchbox reading (Shunt Cap.)	3rd Harmonics	3rd harmonics current	f1I	1st harmonics current	.	.
Source div cap_current_1	Current flowing source coil1	4th Harmonics	4th harmonics current	f1Phase	1st harmonics phase	.	.
Source div cap_current_2	Current flowing source coil2	2nd phase	2nd harmonics current	f2V	2nd harmonics voltage	.	.
.	.	3rd phase	3rd harmonics phase	f2I	2nd harmonics current		
.	.	4th phase	4th harmonics phase	f2Phase	2nd harmonics phase		
.	.			f3V	3rd harmonics voltage		
				f3I	3rd harmonics current		
				f3Phase	3rd harmonics phase		
				f4V	4th harmonics voltage		
				f4I	4th harmonics current		
				f4Phase	4th harmonics phase		
				f5V	5th harmonics voltage		
				f5I	5th harmonics current		
				f5Phase	5th harmonics phase		
80		9		18		1201	

Table 2
Step change test conditions of seven MVs for sensor data acquisition.

MVs	1st step	2nd step	3rd step	4th step	5th step	6th step	7th step	8th step	9th step	10th step	11th step	12th step	13th step	14th step	15th step
Pressure (mT)			10% Up		Baseline										
Source Power (W)					10% Up		Baseline								
Bias Power(W)					Baseline		15% Up		Baseline			Baseline	Baseline		Baseline
Gas1 Flow (sccm)	Stabilize Step	Baseline		Baseline		Baseline		Baseline	10% Up	Baseline				Baseline	
Gas2 Flow (sccm)			Baseline						Baseline		10% Up				
Gas3 Flow (sccm)							Baseline				Baseline		10% Up		
Gas4 Flow (sccm)													Baseline		10% Up

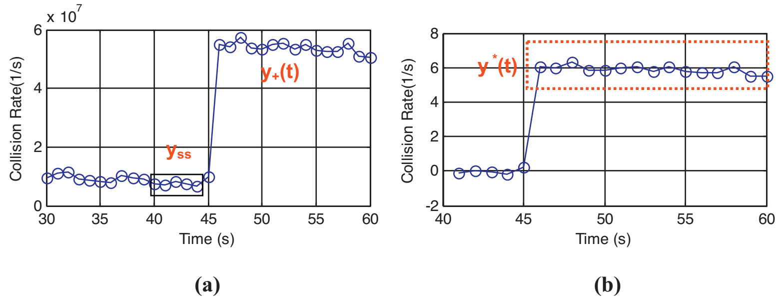

Fig. 4. Signals of collision rate for the step change test of source power: (a) raw signal of collision rate where y_{ss} is the average of steady state data points before step change and $y_+(t)$ is the data point at the time before and after step change and (b) normalized signal, y^*.

Table 3
Top 10 sensor variables based on ISR with regard to source power, bias power and gas 4 flow.

	Source power	ISR	Bias power	ISR	Gas 4 flow	ISR
1	SV 1_S	3.461E+01	SV 1_S	3.549E−01	SV 1_S	1.063E−01
2	SV 1_H	4.936E−01	SV 6_S	5.040E−02	SV 2_S	3.713E−04
3	SV 6_S	1.444E−02	SV 3_V	3.936E−02	SV 17_O	3.155E−04
4	SV 9_O	1.346E−02	SV 2_V	2.097E−02	SV 4_O	1.342E−04
5	SV 13_O	1.156E−02	SV 3_H	2.097E−02	SV 7_O	1.234E−04
6	SV 11_O	1.143E−02	SV 4_S	1.457E−02	SV 6_O	1.229E−04
7	SV 8_O	1.142E−02	SV 4_H	1.045E−02	SV 9_O	1.207E−04
8	SV 3_O	1.075E−02	SV 5_S	9.763E−03	SV 11_S	1.161E−04
9	SV 1_V	1.022E−02	SV 3_S	7.347E−03	SV 14_O	1.142E−04
10	SV 10_O	9.968−03	SV 5_V	5.878E−03	SV 10_O	1.130E−04

Note: _S denotes a sensor variable from SEERS; _O denotes a sensor variable from OES, _V denotes a sensor variable from VI-probe; _H denotes a sensor variable from hardware gauge group.

step change test is done on the same condition, a step with the baseline condition before and after the step change test is inserted. The step time is determined long enough to reach steady state, which is monitored by plasma parameters such as electron collision rate and electron density from SEERS.

Since each steady state sensor response shows strong, moderate or weak response to the step change of MVs, a numerical criterion, integrated squared response (ISR), is developed for their classification. Fig. 4 shows how ISR is calculated from a raw sensor signal after a step change test. The raw signal of collision rate from SEERS, which measures electron collision frequency in plasma, shows significant response to a 10% change of source power at 46 s and reaches steady state in a few seconds. The raw signal of collision rate is then normalized by using Eq. (1):

$$y^* = \frac{(y_+(t) - y_{ss})}{y_{ss}} \tag{1}$$

where y_{ss} is the average of steady state data points before the step change and $y_+(t)$ is the data point at the time before and after the step change.

This normalization by Eq. (1) solves scaling issues in plasma etching, which is described in Section 2.3 and the first paragraph of Section 3.1. The normalized data, y^*, are then integrated from the start to the end of the step change for the ISR calculation:

$$\text{ISR} = \frac{1}{b-a}\int_a^b (y^*(t))^2\,dt \tag{2}$$

where a and b are the start of step change and the end time of step change, respectively.

Table 3 lists a part of sensor variable ranking table for source power, bias power, and the flow rate of Gas 4, based on ISR. For source power, two variables from SEERS, six variables from OES, one variable from VI-probe, and one variable from the hardware gauge group are selected as the top ten important sensor variables. This result is thought to be reasonable, given that all of the selected variables are related to the properties of electron, ion and etchant in the plasma. In the bias power case, five variables from SEERS, three variables from VI-probe, and two variables from hardware gauges are selected, but no variables from OES are included in the list. This result is also plausible, given that bias power does not impact etchant very much and both VI-probe and the selected hardware gauges measure rf properties of bias power. For the flow rate of Gas 4, seven variables from OES and three variables from SEERS are in the top ten sensor variable list. This is also thought to be a reasonable result, given that OES and SEERS can measure chemical properties of plasma that is changed by increasing gas flow rate. Thus it is thought that sensor ranking based on ISR reflects intuitive physical and chemical properties of sensor variables.

3.2. Incorporation with relative gain array (RGA) method for enhancing the ISR based variable selection

Determining an optimum sensor variable set is still challenging even with the ISR based sensor ranking table because there are complex interactions between SVs and MVs in plasma etching. Therefore, interaction analysis between SVs and MVs is needed to make in order to enhance the performance of the ISR based sensor variable selection method.

The relative gain array (RGA) originated by Bristol is a useful tool to analyze interactions between input and output variables in multiple input-multiple output (MIMO) control systems. One or more MVs can affect the interactions of controlled variables (CVs) in a specific loop or all other control loops. Therefore, understanding the dependence of different MVs and CVs in the control scheme could be extremely helpful in designing and implementing a control scheme for a process.

If a control system with n controlled variables and n manipulated variables exists, the relative gain λ_{ij} between a controlled variable, y_i, and a manipulated variable, u_j, is defined to be the dimensionless ratio of two steady-state gains:

$$\lambda_{ij} = \frac{(\partial y_i/\partial u_j)_u}{(\partial y_i/\partial u_j)_y} = \frac{\text{open-loop gain}}{\text{closed-loop gain}} \tag{3}$$

for $i = 1, 2, \ldots, n$ and $j = 1, 2, \ldots, n$.

In Eq. (3), the symbol, $(\partial y_i/\partial u_j)_u$, denotes a partial derivative that is evaluated with all of the manipulated variables except u_j held constant. Thus this term is the open-loop gain between y_i and u_j. Similarly, $(\partial y_i/\partial u_j)_y$ can be interpreted as a closed-loop gain that indicates the effect of u_j and y_i when all of the other feedback control loops are closed.

The RGA, denoted by Λ, is defined as follows:

$$\Lambda = \begin{array}{c} \\ y_1 \\ y_2 \\ \cdots \\ y_n \end{array} \begin{array}{c} \begin{array}{cccc} u_1 & u_2 & \cdots & u_n \end{array} \\ \begin{bmatrix} \lambda_{11} & \lambda_{12} & \cdots & \lambda_{1n} \\ \lambda_{21} & \lambda_{22} & \cdots & \lambda_{2n} \\ \cdots & \cdots & \cdots & \cdots \\ \lambda_{n1} & \lambda_{n2} & \cdots & \lambda_{nn} \end{bmatrix} \end{array} \tag{4}$$

The RGA has some important properties and guidelines to understand and utilize it (Seborg, Edgar, & Mellichamp, 2003).

(1) It is normalized because the sum of the elements in each row or column is equal to one.
(2) The relative gains are dimensionless and thus not affected by choice of units or scaling of variables.
(3) The RGA is a measure of sensitivity to element uncertainty in the process gain matrix K. The gain matrix can become singular if a single element K_{ij} is changed to $K_{ij} = K_{ij}(1 - 1/\lambda_{ij})$. Thus a large RGA element indicates that small changes in K_{ij} can noticeably change the process control characteristics.
(4) if $\lambda_{ij} = 0$, the manipulated variable, u_j, will have no effect on the output controlled variable, y_i.
(5) if $\lambda_{ij} = 1$, the manipulated variable, u_j, affects the output, y_i, without any interaction from the other control loops in the system. From the definition of λ_{ij}, this implies that the gain loop with all loops open is equal to the gain loop with all other loops closed.
(6) if $\lambda_{ij} < 0$, the system will be unstable whenever u_j is paired with y_i, and the opposite response in the actual system may occur if other loops are opened in the system.
(7) if $0 < \lambda_{ij} < 1$, other control loops $(u_j - y_i)$ are interacting with the manipulated and controlled variable control loop.

According to the RGA properties, there are two rules to pair controlled and manipulated variables. The first rule is to choose the RGA row element that is close to unity and the second rule is to avoid negative elements.

The RGA method has been extended to non-square systems by Chang and Yu. For a non-square system with more outputs than inputs $(m > n)$, it is not possible to keep all outputs at their points. Therefore, the sense of perfect control in the definition of closed-loop gain should be modified. In this sense, a perfect control in the least-square sense is proposed. That is, a controller is designed such that the steady-state offsets are minimized in the sense of least square. Then the non-square relative gain array (NRGA) is calculated as follows:

$$\Lambda^{N} = K \otimes (K^{+})^{T} \tag{5}$$

where Λ^N is the non-square relative gain array, and $\otimes$ denotes element by element multiplication, and K is the non-square gain matrix between CVs and MVs, and K^+ is the pseudo, or Moore–Penrose, inverse of K.

The NRGA method has the similar properties to those of RGA method except that the sum of the elements in each row of the NRG falls between zero and unity. It follows the same input-output pairing rules as those of the RGA, but due to the control in the least-square sense, the sum of squared errors (SSE) caused by uncontrolled SVs should be investigated.

The SSE for the entire system under perfect control of a selected square sub-system can be calculated as follows. If there is a $(m \times n)$ $(m > n)$ non-square system with its transfer function matrix G and n outputs for control are chosen, the system can be partitioned into

$$\begin{bmatrix} y_S \\ --- \\ y_R \end{bmatrix} = \begin{bmatrix} G_S \\ --- \\ G_R \end{bmatrix} u \tag{6}$$

where y_S is a $(n \times 1)$ output vector for the selected (controlled) outputs and y_R is a $((m-n) \times 1)$ output vector for the remaining (uncontrolled) outputs.

When considering steady-state error only, the input vector for the square sub-system in closed-loop is calculated by

$$\bar{u} = G_S^{-1} \bar{y}_S^{set} \tag{7}$$

where a pseudo inverse of G_s is employed when the inverse of G_s does not exist.

When the square sub-system is under perfect control, the steady-state error for all output is described by

$$\bar{e} = (I_{m\times n}^{N} - G G_S^{-1}) \bar{y}_S^{set} \tag{8}$$

where $I_{m\times n}^{N}$ is a $(m \times n)$ matrix with unity in the diagonal and zero elsewhere, and $\bar{e}$ is a $(m \times 1)$ steady-state error vector.

Thus for a particular choice of the square sub-system, G_s, the SSE is defined as

$$SSE = \sum_{i=1}^{n} \left\| \bar{e}(i) \right\|_2^2 = \sum_{i=1}^{n} \left\| (I_{m\times n}^{N} - G G_S^{-1}) \bar{y}_{S,i}^{set} \right\|_2^2 \tag{9}$$

where $\bar{y}_{S,i}^{set}$ is $(n \times 1)$ vector with unity in the ith entry and zero elsewhere, and $\bar{e}(i)$ is $(m \times 1)$ steady state error vector corresponding to the specific input $\bar{y}_{S,i}^{set}$, and G_s is the steady state gain of square sub-system.

4. Application to critical dimension (CD) virtual metrology (VM) in plasma etching

4.1. Virtual metrology in semiconductor manufacturing

VM is a technique to estimate wafer metrology variables using in situ sensor measurements, where there is a regression model between SVs as input and PVs as output. Due to its capability to provide wafer-to-wafer quality assurance, VM has been attracting much interest in recent years from semiconductor manufacturers and researchers (Chen et al., 2005; Hung, Lin, Cheng, & Lin, 2007; Imai & Kitabata, 2009; Kang et al., 2009; Khan, Moyne, & Tilbury, 2008; Lynn, Ringwood, Ragnoli, Mcloone, & MacGearailt, 2009; Lynn, MacGearailt, & Ringwood, 2012; Vitale et al., 2008; Zeng & Spanos, 2009). A well-developed VM system can reduce requirements for physical metrology, which adds to the cost and is a bottleneck in semiconductor manufacturing. VM provides real-time quality assurance for production tools instead of scheduled tool monitoring with test wafers. In addition, VM can be incorporated into wafer-to-wafer process control strategies, which can mitigate measurement delay issues (Kang, Kim, Lee, Doh, & Cho, 2011; Khan et al., 2008).

Building a VM system in plasma etching starts from input variable selection for an output variable such as CD, etched depth, or etch rate. However, since plasma etch processes have a large number of SVs from sensors as described in Section 2.2, selecting proper input variables that are better correlated with output variables is always challenging when implementing a reliable VM system. In addition, the number of selected input variables should be minimized, given that the cost for computer resources to maintain a

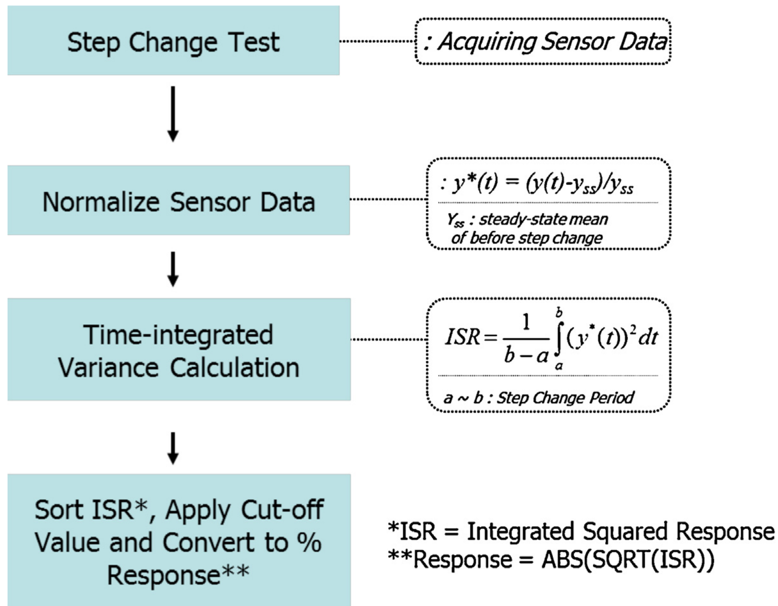

Fig. 5. A procedure for constructing a reference sensor library through ISR based sensor selection method.

fab-wide VM system can increase with the number of input variables. Therefore, variable selection is an important step in building a VM system as a starting point. For this reason, many statistical approaches have been tried for variable selection (Kang et al., 2011; Lin, Cheng, Ye, Wu, & Hung, 2008; Lynn et al., 2009; White et al., 2000; Wise, Gallagher, Butler, White, & Barna, 1999). Those statistical approaches may be useful in handling a large number of variables, but relying on statistical methods only without consideration of the physical meanings of variables may exclude important variables. In addition, the result that a VM system in plasma etching shows much more reliable performances by selecting important plasma variables (Kim, Baek, Kim, Choi, & Han, 2007) underscores the consideration of physical properties on variables in selecting input variables. Under these circumstances, new variable selection approach that can reflect physical meanings of variables is needed to develop for a reliable and cost-effective VM system.

4.2. Constructing reference sensor library for each MV

Since the entire sensor response to each MV can be numerically ranked on the basis of the ISR, it becomes easy to construct a reference sensor library for each MV. Fig. 5shows a procedure for constructing the reference sensor library. After acquiring all sensor data for each MV by running the recipe in Table 2, response of the sensor variables toward each MV are numerically analyzed by the ISR. Since each sensor has its own ISR value for a particular MV, all of the sensor variables can be sorted in a descending order of the ISR value.

Table 4 is a part of that reference sensor library in which sensor variables are categorized into three groups (1: strong, 0.5: moderate, and 0: weak responses to each MV).

According to the reference sensor library, SV 1_S from SEERS is the most sensitive variable in this plasma etching system, which strongly responds to various MVs from source power to gas 4 flow. In addition, sensor variables from OES are the most sensitive especially to pressure in our plasma process condition. Other sensor variables form hardware gauges and VI-probe do not appear as the top sensitive sensor variables in Table 4 even though some of sensor variables from them are the most sensitive to particular MV.

The reference sensor library facilitates an accurate and fast fault diagnosis even without additional knowledge of plasma sensors. For example, once a fault is alarming by violating a statistical process control (SPC) limit of SV 1_S in Table 4, which strongly responds to various MVs from source power to gas 4 flow, taking a look at other SV's responses enables us to efficiently find the malfunctioned MV which is difficult to be detected in built-in hardware gauges. This procedure can be implemented without any difficulties in a fault detection system in which various algorithms to match sensor variable patterns are equipped. In addition, this reference sensor library can provide insight on plasma state sensor variables for engineers so that they can utilize the plasma sensor variables

Table 4
A part of the reference sensor library for seven MVs made by the ISR-based variable selection method.

MVs	Sensor variables											
	SV 1_S	SV 2_S	SV 4_O	SV 7_O	SV 14_O	SV 15_O	SV 9_O	SV 11_O	SV 1_O	SV 2_O	SV 4_S	SV 5_S
Pressure	0	0	1	1	1	1	1	1	1	1	0	0
Source power	1	1	1	1	1	1	1	1	1	1	1	1
Bias power	1	1	0	0	0	0	0	0	0	0	1	1
Gas 1 flow	1	1	1	1	1	1	1	1	1	1	1	1
Gas 2 flow	1	1	1	1	1	1	1	1	1	1	0	0
Gas 3 flow	1	1	0.5	0.5	0.5	0.5	0	0	0	0	1	1
Gas 4 flow	1	0	0.5	0.5	0.5	0.5	0.5	0.5	0	0	0	0
Sum	6	5	5	5	5	5	4.5	4.5	4	4	4	4

Note: 1 means strong response (ISR value > 0.01), 0.5 means moderate strong response (0.0025 < ISR value < 0.01), and 0 means weak response (ISR value < 0.0025).

Table 5
The calculated NRGA of the 18 × 7 steady-state gain matrix.

	Pressure	Source power	Bias power	Gas 1 flow	Gas 2 flow	Gas 3 flow	Gas 4 flow
SV 1	0.000	−0.019	0.138	0.560	0.651	−0.284	−0.047
SV 2	0.588	−0.362	0.000	−0.435	0.314	0.108	−0.074
SV 3	**0.624**	−0.381	0.000	−0.513	0.406	0.142	−0.122
SV 4	0.402	−0.273	0.000	−0.388	0.333	0.102	−0.043
SV 5	−0.235	0.185	0.000	0.229	−0.129	−0.054	0.105
SV 6	−0.884	**0.783**	0.000	**0.982**	−0.702	−0.194	0.311
SV 7	0.466	−0.310	0.000	−0.420	0.388	0.143	−0.119
SV 8	0.037	−0.046	0.000	−0.053	0.120	0.029	0.027
SV 9	−0.021	0.031	0.000	0.033	−0.004	−0.009	0.047
SV 10	0.755	−0.469	0.000	−0.659	0.509	0.149	−0.094
SV 11	0.000	0.180	**0.349**	0.000	−0.670	0.162	**0.972**
SV 12	0.157	−0.055	0.000	−0.047	0.023	0.032	−0.040
SV 13	−1.289	**1.358**	0.000	1.455	−1.103	−0.283	0.433
SV 14	−0.198	0.446	−0.013	−0.222	**0.593**	−0.156	0.014
SV 15	0.000	−0.077	**0.338**	0.329	0.106	0.493	−0.202
SV 16	0.236	0.087	0.000	−0.020	0.165	−0.046	−0.067
SV 17	0.000	0.020	0.185	0.169	0.000	**0.625**	0.000
SV 18	0.362	−0.100	0.003	0.000	0.000	0.042	−0.102

Table 6
The top 10 square sub-systems having lowest SSEs.

Square sub-system	1	2	3	4	5	6	7	8	9	10
Selected SVs	SV 1 SV 10 SV 11 SV 13 SV 14 SV 15 SV 17	SV 1 SV 10 SV 11 SV 13 SV 15 SV 16 SV 17	SV 1 SV 3 SV 11 SV 13 SV 14 SV 15 SV 17	SV 1 SV 7 SV 11 SV 13 SV 14 SV 15 SV 17	SV 1 SV 6 SV 10 SV 11 SV 14 SV 15 SV 17	SV 1 SV 2 SV 11 SV 13 SV 14 SV 15 SV 17	SV 1 SV 3 SV 11 SV 13 SV 15 SV 16 SV 17	SV 1 SV 4 SV 11 SV 13 SV 14 SV 15 SV 17	SV 1 SV 7 SV 11 SV 13 SV 15 SV 16 SV 17	SV 1 SV 4 SV 11 SV 13 SV 15 SV 16 SV 17
SSE	9.975	10.142	10.166	10.304	10.308	10.313	10.330	10.350	10.367	10.445

effectively when setting up a process, building a VM model, and controlling equipment.

4.3. Selecting input variables for virtual metrology in plasma etching

When building a VM model, the input variables should be selected and optimized to minimize the bad effects described in Section 3.1. As one of the most commonly used method for variable selection, stepwise regression has been utilized in various VM cases (Chen et al., 2005; Khan et al., 2008; Lin et al., 2008). It includes regression models in which the choice of predictive variables is made in an automatic procedure which is based on statistics such as *F*-tests, *t*-tests, adjusted *R*-square and so on (Hocking, 1976). However, there are some criticisms on the stepwise regression in the sense that relying on statistics only might lead to wrong decisions (Cook & Weisberg, 1999; Good & Hardin, 2003). Specifically, in plasma etching where nonlinear behavior of plasma governs reaction of process, physical properties of each sensor should be understood before running statistic based variable selection methods. In addition, the effect of scaling of variables should be minimized.

Since the process results are closely related to SVs and the SVs are manipulated by MVs, selecting SVs corresponding to MVs might be a proper approach to determining an optimum input variable set for VM. Specifically, selecting at least one SV per MV is desirable for controller robustness. In this sense, the reference sensor library in Section 4.2 is definitely useful because it allows engineers to select proper SVs which is sensitive to MVs.

Determining an optimum input variable set is still challenging even with the reference sensor library because there are complex interactions between SVs and MVs in plasma etching. Therefore, interaction analysis between SVs and MVs should be considered in selecting an optimum input variable set. For this purpose, the RGA method described in Section 3.2 is incorporated with the ISR-based sensor variable selection technique.

In order to determine optimum input variable sets for VM, the systematic variable selection in which the ISR-based sensor variable selection and NRGA is incorporated is made. As a first step, MVs which are effective to control CD are determined based on engineers' knowledge. Then top ranked sensor variables for each MV are chosen, which can be obtained in the reference sensor library in Section 4.2. The number of top sensor variables per MV is determined, considering the total number of MVs. Then, sensor variables with zero steady-state gain elements for several MVs are excluded because the SV with zero gain for a MV implies that it does not respond to the particular MV. After that, NRGA of the steady-state gain matrix between MVs and SVs is calculated through Eq. (5). Table 5 summarizes the NRGA of (18 × 7) steady-state gain matrix, where the relative gains of each MV which are close to unity as much as possible are in bold.

According to the RGA rules in Section 3.2, possible MV-SV pairings can be determined as follows: (Pressure – SV 3 or SV 10), (Source Power – SV 6 or SV 13), (Bias Power – SV 11 or SV 15), (Gas 1 Flow – SV6), (Gas 2 Flow – SV1 or SV14), (Gas 3 Flow – SV 17), and (Gas 4 Flow – SV11).

These selected possible pairings by the RGA rules is not always valid for non-square systems (Chang & Yu, 1990), so the sum of squared errors (SSE) caused by uncontrolled SVs should be investigated for all possible (7 × 7) square sub-systems. Table 6 summarizes the top ten square sub-systems having lowest SSEs, which is calculated by Eq. (9). The top square sub-system consists of SV 1, SV 10, SV 11, SV 13, SV 14, SV 15, and SV 17. These selected SVs are a part of the selected nine SVs through the RGA rules above. The other square sub-systems in Table 6 also include at least six SVs matching the selected SVs through the RGA rules. This suggests the selected SVs through the RGA rules are also valid for the non-square system.

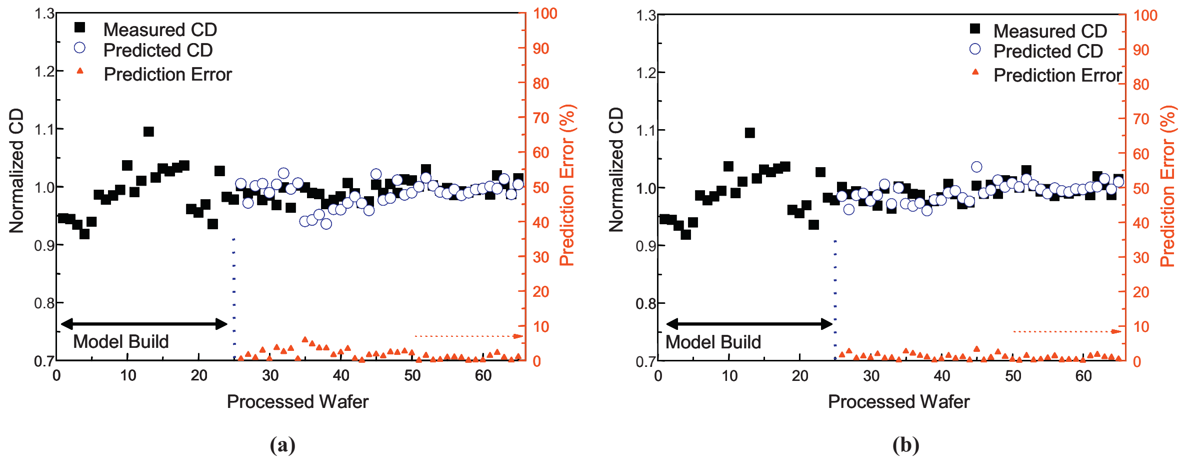

Fig. 6. Metal line CD prediction performance of VM systems: (a) MLR and (b) PLSR are applied to build the VM model.

4.4. Implementing a reliable VM system by simple linear regression methods

With the top square sub-system selected in Section 4.3, VM models to predict a metal line critical dimension (CD) in a DRAM device is built by applying simple linear regression methods such as multiple linear regression (MLR) and partial least squares regression (PLSR). Since an optimum input variable set which is closely related to each MVs and reflects physical properties of plasmas is selected, it is believed that a robust VM model without employing more complex regression methods such as neural network (Johannesmeyer, Singhai, & Serborg, 2002) and support vector regression (SVR) (Smola & Schölkopf, 2004) could be built.

Fig. 6 shows the performance of the VM systems built with MLR and PLSR methods. 25 wafers are prepared for VM model construction, some of which have a CD value larger than the normal specification and the other 40 wafers under normal operations are utilized for the performance check of the VM systems. The prediction error of both models is less than 5% if several outliers which come from sources other than VM itself are excluded. The mean absolute percentage error (MAPE) of the VM system is larger than other published VM results (Lin et al., 2008; Lynn et al., 2009) but considering that the VM system in this paper predicts much more tricky CD than etch rate or etched depth in those papers and furthermore the number of input variables employed in the VM model is relatively small, the ISR based sensor variable selection method introduced in this paper is worthwhile. In addition, it might be the first results to implement the robust CD VM with less than 10 input variables in plasma etching.

5. Conclusions

Because plasma etching processes have a large number of state variables (SVs) to be utilized, and the number of possible SVs is continually growing, an effective sensor variable selection technique is necessary. The time-integrated variance calculation method introduced in this paper can be a proper approach to handling a large number of sensors. Based on integrated squared response (ISR) obtained through the time-integrated variance calculation of sensor data from step change tests, sensor variables can be ranked with regard to particular manipulated variables (MVs), which can be utilized to make ISR-based sensor variable tables and a reference sensor library. With the ISR-based sensor variable tables and the reference sensor library, process and equipment engineers can gain insight into physical behavior of complicated plasma sensors and can facilitate wafer-to-wafer quality assurance. Strengths and benefits of optimum sensor variable selection combined with physical interpretation of sensor properties are successfully demonstrated by building a virtual metrology (VM) system predicting metal line critical dimension (CD) for a dynamic random access memory (DRAM). We hope that the results introduced in this paper encourage development of more affordable and general sensor variable selection techniques for process and equipment engineers in plasma etching.

Acknowledgements

The authors would like to thank Quentin E. Walker and Xiaoliang Zhuzng from Applied Materials for their technical support.

References

Baek, K. H., Jung, Y., Min, G. J., Kang, C., Cho, H. K., & Moon, J. T. (2005). Chamber maintenance and fault detection technique for a gate etch process via self-excited electron resonance spectroscopy. *Journal of Vacuum Science and Technology B*, *23*(1), 125–129.

Chang, J., & Yu, C. C. (1990). The relative gain for non-square multivariable systems. *Chemical Engineering Science*, *45*(5), 1309–1323.

Chen, R., Huang, H., Spanos, C. J., & Gatto, M. (1996). Plasma etch modeling using optical emission spectroscopy. *Journal of Vacuum Science and Technology A*, *14*(3), 1901–1906.

Chen, P., Wu, S., Lin, J., Ko, F., Lo, H., Wang, J., et al. (2005). Virtual metrology: A solution for wafer to wafer advanced process control. In *International Symposium on Semiconductor Manufacturing* San Jose, CA, USA, (pp. 155–156).

Coburn, J. W., & Chen, M. (1980). Optical emission spectroscopy of reactive plasmas: A method for correlating emission intensities to reactive particle density. *Journal of Applied Physics*, *51*(6), 3134–3136.

Cook, R. D., & Weisberg, S. (1999). *Applied regression including computing and graphics*. New York: Wiley.

Good, P. I., & Hardin, J. W. (2003). *Common errors in statistics (and how to avoid them)*. New Jersey: Wiley.

Hocking, R. R. (1976). The analysis and selection of variables in linear regression. *Biometrics*, *32*, 1–49.

Hung, M. H., Lin, T. H., Cheng, F. T., & Lin, R. C. (2007). A novel virtual metrology scheme for predicting CVD thickness in semiconductor manufacturing. *IEEE/ASME Transactions on Mechatronics*, *12*(3), 308–316.

Imai, S. I., & Kitabata, M. (2009). Prevention of copper interconnection failure in system on chip using virtual metrology. *IEEE Transactions on Semiconductor Manufacturing*, *22*(4), 432–437.

Johannesmeyer, M. C., Singhai, A., & Serborg, D. E. (2002). Pattern matching in historical data. *AIChE Journal*, *48*, 2022–2038.

Jolliffe, I. T. (2002). *Principal component analysis* (2nd ed.). Springer-Verlag New York, Inc.

Kang, P., Kim, D., Lee, H. J., Doh, S., & Cho, S. (2011). Virtual metrology for run-to-run control in semiconductor manufacturing. *Expert Systems with Applications*, *38*, 2508–2522.

Kang, P., Lee, H. J., Cho, S., Kim, D., Park, J., Park, C. K., et al. (2009). A virtual metrology system for semiconductor manufacturing. *Expert Systems with Applications*, *36*, 12554–12561.

Khan, A. A., Moyne, J. R., & Tilbury, D. M. (2008). Virtual metrology and feedback control for semiconductor manufacturing processes using recursive partial least squares. *Journal of Process Control*, *18*, 961–974.

Klick, M. (1996). Nonlinearity of the radio-frequency sheath. *Journal of Applied Physics*, *79*(7), 3445–3452.

Klick, M., Rehak, W., & Kammeyer, M. (1997). Plasma diagnostics in rf discharges using nonlinear and resonance effects. *Japanese Journal of Applied Physics Part 1*, *36*(7B), 4625–4631.

Kim, Y. J., Baek, K. H., Kim, Y. J., Choi, S. W., & Han, W. S. (2007). In-situ plasma monitoring and virtual metrology via SEERS in dielectric etch. In *8th European AEC/APC conference* Dresden, Germany.

Lieberman, M. A., & Lichtenberg, A. J. (2005). *Principles of plasma discharges and materials processing*. New Jersey: John Wiley & Sons, Inc.

Lin, T. H., Cheng, F. T., Ye, A. J., Wu, W. M., & Hung, M. H. (2008). A novel key variable sifting algorithm for virtual metrology. In *IEEE international conference on robotics and automation* Pasadena, CA, USA, (pp. 3636–3641).

Lynn, S. A., MacGearailt, N., & Ringwood, J. V. (2012). Real-time virtual metrology and control for plasma etch. *Journal of Process Control*, *22*, 666–676.

Lynn, S. A., Ringwood, J. V., Ragnoli, E., Mcloone, S., & MacGearailt, N. (2009). Virtual metrology for plasma etch using tool variables. In *IEEE/SEMI Advanced Semiconductor Manufacturing Conference* Berlin, Germany, (pp. 143–148).

Park, H. M., Grimard, D. S., & Grizzle, J. W. (2003). Sensor fault detection in etch based on broadband rf signal observation. *Journal of Vacuum Science and Technology A*, *21*(3), 814–824.

Seborg, D. E., Edgar, T. F., & Mellichamp, D. A. (2003). *Process Dynamics and Control*. New York: Wiley.

Semmler, E., Awakowicz, P., & Keudell, A. (2007). Heating of a dual frequency capacitively coupled plasma via the plasma series resonance. *Plasma Sources Science and Technology*, *16*(4), 839–848.

Smola, A. J., & Schölkopf, B. (2004). A tutorial on support vector regression. *Statistics and Computing*, *14*(3), 199–222.

Sobolewski, M. A. (2006). Real-time, noninvasive monitoring of ion energy and ion current at a wafer surface during plasma etching. *Journal of Vacuum Science and Technology A*, *24*(5), 1892–1905.

Vitale, V., Aderhold, W., Hunter, A., Iliopoulos, I., Kroupnova, N., Yanovich, A., et al. (2008). Use of virtual metrology for in-situ visualization of thermal uniformity and handoff adjustment in RTP critical anneals. In *IEEE/SEMI Advanced Semiconductor Manufacturing Conference* Cambridge, MA, USA, (pp. 349–353).

Wise, B. M., Gallagher, N. B., Butler, S. W., White, D. D., Jr., & Barna, G. G. (1999). A comparison of principal component analysis, multiway principal component analysis, trilinear decomposition and parallel factor analysis for fault detection in a semiconductor etch processes. *Journal of Chemometrics*, *13*, 379–396.

White, D., Goodlin, B., Gower, A., Boning, D., Chen, H., Sawin, H., et al. (2000). Low open-area endpoint detection using a PCA-based T^2 statistics and Q statistic on optical emission spectroscopy measurements. *IEEE Transactions on Semiconductor Manufacturing*, *13*(2), 193–207.

Wold, S., Esbensen, K., & Geladi, P. (1987). Principal component analysis. *Chemometrics and Intelligent Laboratory Systems*, (2), 37–52.

Yue, H. H., Qin, S. J., Markle, R. J., Nauert, C., & Gatto, M. (2000). Fault detection of plasma etchers using optical emission spectra. *IEEE Transactions on Semiconductor Manufacturing*, *13*(3), 374–385.

Zeng, D., & Spanos, C. J. (2009). Virtual metrology modeling for plasma etch operations, spectra. *IEEE Transactions on Semiconductor Manufacturing*, *22*(4), 419–431.